Effect of Nutraceuticals on Adult MSCs

Figure 1:

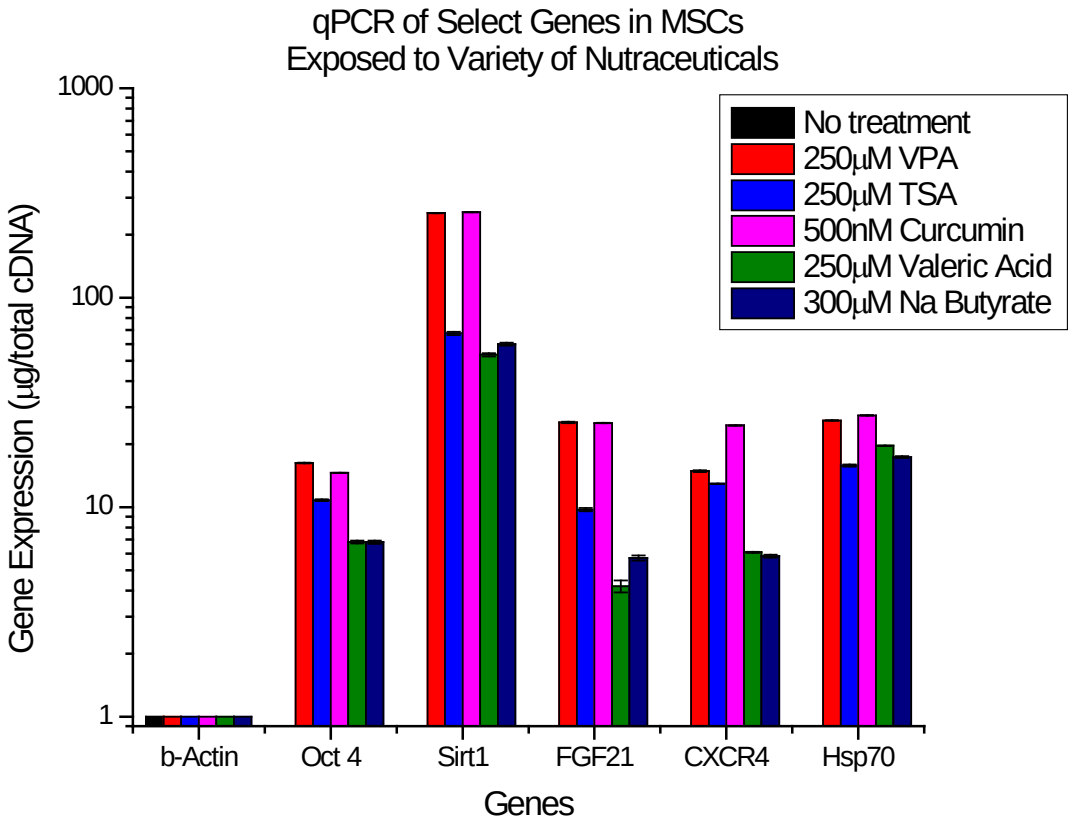

In Figure 1, results of gene expression analysis are shown following the exposure of MSCs to varying nutraceuticals. Figure 1 is a bar graph representation illustrating PCR used to measure target genes known to be subject to epigenetic regulation by both HDAC inhibitors. The graph shows the result of human MSCs treated with varying nutraceuticals alone. The expression of Oct 3/4, a well-known pluripotency gene, was increased about 20-fold compared to untreated human MSCs. The expression of SIRT-1 was highly elevated compared to untreated MSC by ~300-fold without differences between treatment with either VPA or Curcumin. The expression of FGF-21 was also elevated by 25-fold and its expression was higher in MSCs treated with VPA or Curcumin, although this increase is not significant. CXCR4 expression was highest in Curcumin treated MSCs, which is a well-known marker of stem cell migration activity. The expression of Hsp70 was elevated by 25-fold and its expression was highest in MSCs treated with VPA and Curcumin, but not significant. All gene

expression was normalized to untreated MSCs. Beta actin was measured as a house-keeping gene. The graph shows the result of gene expression analysis of human MSCs treated with varying nutraceuticals compared to VPA. Gene expression was quantified by determining the amount of gene-specific DNA/total cDNA. Data is mean +/- SD of 4 replicates. These results thus show highest increased expression of Oct 3/4, SIRT-1, FGF-21, CXCR4, and Hsp70 as a result of exposure to 250µM VPA and 500nM Curcumin.

Native human cord blood-derived MSCs (Vitro Biopharma Cat. No. SC00A1) were expanded from cryopreservation in a T-25 TC-coated flasks (BD Falcon, Cat. No. 353108) in MSC-Gro™ low serum, complete medium (Vitro Biopharma Cat. No. SC00B1). Cells were sub-cultured and counted on a Beckerman-Coulter Z2 particle counter (range 10 µm-30 µm). Cells were plated at 10,000/cm^2 a TC-coated Greiner Bio-One T75 flask and maintained in MSC-Gro™ serum free, complete medium (Vitro Biopharma Cat. No. SC00B3) in a reduced O_2 environment (1%O_2, 5%CO_2, 94%N_2) at 37ºC in a humidified chamber. The MSCs were treated continuously for up to 2 weeks. Cultures were fed every three days. Cells were harvested using Accutase (Innovative Cell Technologies Inc., Cat No AT-104) and centrifuged (450 x g) for 7 minute. Cell supernatant was aspirated off and cells were resuspended in 1mL PBS and counted on a Beckerman-Coulter Z2 particle counter (range 10 µm-30 µm).

Total RNA was extracted using RNeasy Mini Kit (Qiagen Cat. No. 74104). RNA was quantified using an absorbance measurement at 260nm. RNA was converted to cDNA using Quantitect Reverse Transcription Kit (Qiagen Cat. No.205310) in a thermocycler. RNA was incubated in the gDNA elimination reaction for 2 minutes at 42ºC then incubated in the reverse-transcription master mix for 15 minutes at 42ºC. Immediately after, it was incubated at 95ºC for 3 minutes for inactivation. cDNA was sent to an outside lab (CU-Anschutz Metabolic Laboratory) for q-PCR to detect relative or absolute gene expression levels. cDNA was diluted 1:5 and iTaq Universal Supermix fluorescent probe (BioRad Cat. No. 172-5120) used to detect the threshold cycle (Ct) during PCR. Dilution factors and cDNA concentrations were calculated into recorded values then normalized to untreated hMSCs (Vitro Biopharma Cat. No. SC00A1).

Figure 2:

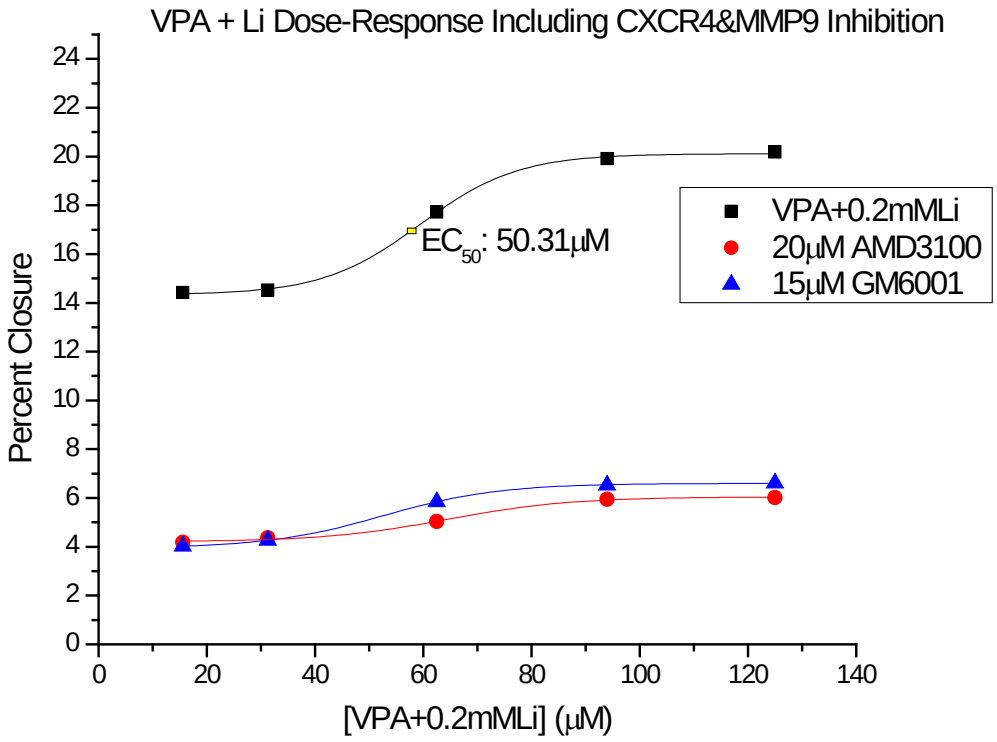

Figure 2 is a line graph representation illustrating migration of CB-MSCs induced by exposure to VPA and 0.2mM lithium (black sqaures), VPA and 0.2mM lithium inhibited by CXCR4 inhibitor (AMD3100) (red circles) and VPA and 0.2mM lithium inhibited by MMP9 inhibitor (GM6001) (blue triangles). Percent closure is plotted as a function of dose and the data was modeled by sigmoidal curve fitting to calculate EC_{50} values. This Figure 2 shows VPA and lithium-induced MSC migration with a calculated EC_{50} of 50.31 µM and maximal migration of the combination of VPA and lithium. The CXCR4 inhibitors showed inhibition of CB-MSC with a closure of 2%. The MMP9 inhibitors also showed inhibition of CB-MSC with a closure of 2%. The results showed a lower EC_{50} than that observed with VPA only, i.e., 32.96 µM (Figure 5) suggesting a synergistic effect of Li-VPA on CB-MSC migration.

Figure 3

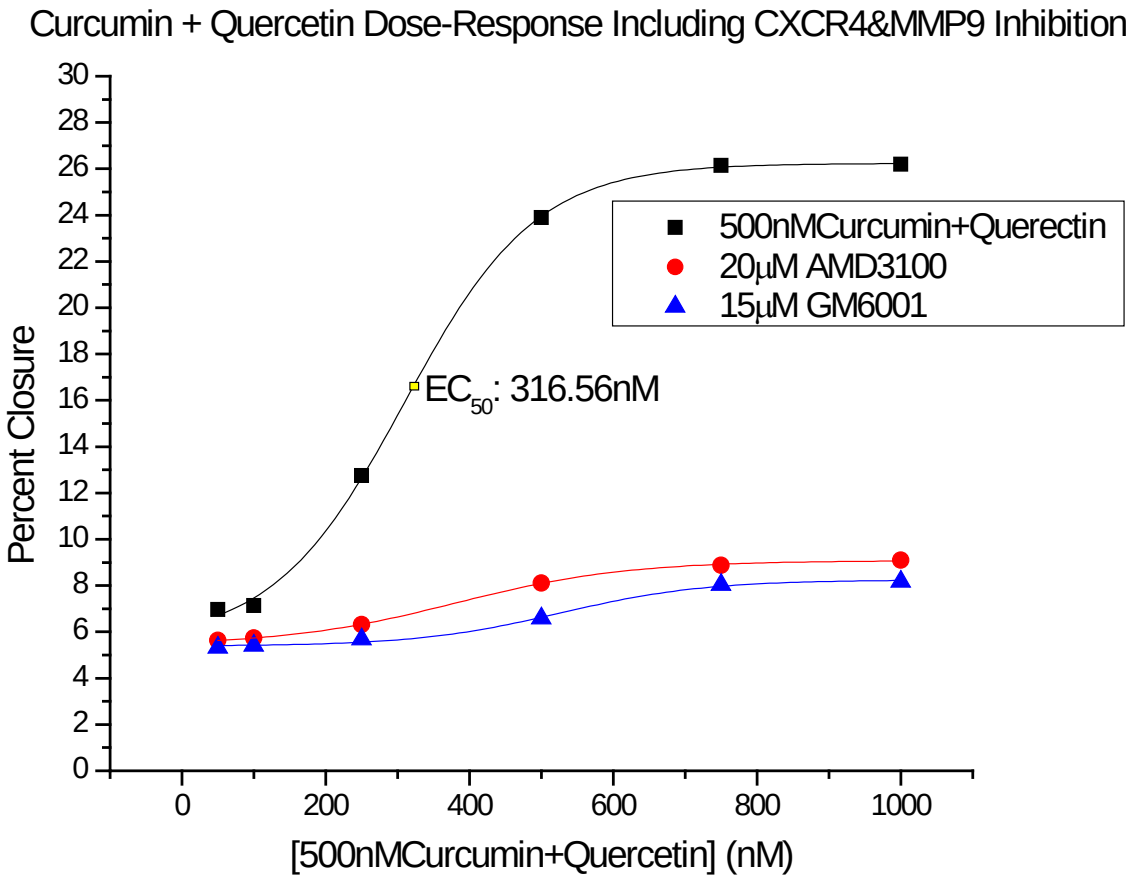

Figure 3 is a line graph representation illustrating migration of CB-MSCs induced by exposure to 500nM curcumin and querectin (black sqaures), 500nM curcumin and querectin inhibited by CXCR4 inhibitor (AMD3100) (red circles) and 500nM curcumin and querectin inhibited by MMP9 inhibitor (GM6001) (blue triangles). Percent closure is plotted as a function of dose and the data was modeled by sigmoidal curve fitting to calculate EC_{50} values. This Figure 3 shows curcumin and querectin-induced MSC migration with a calculated EC_{50} of 316.56 nM and maximal migration of the combination of curcumin and querectin. The CXCR4 inhibitors showed inhibition of CB-MSC with a closure of 2%. The MMP9 inhibitors also showed inhibition of CB-MSC with a closure of 2%. The results showed a lower EC_{50} than that observed with VPA only, i.e., 32.96 µM suggesting a synergistic effect of CC-Quer on CB-MSC migration.

Figure 4:

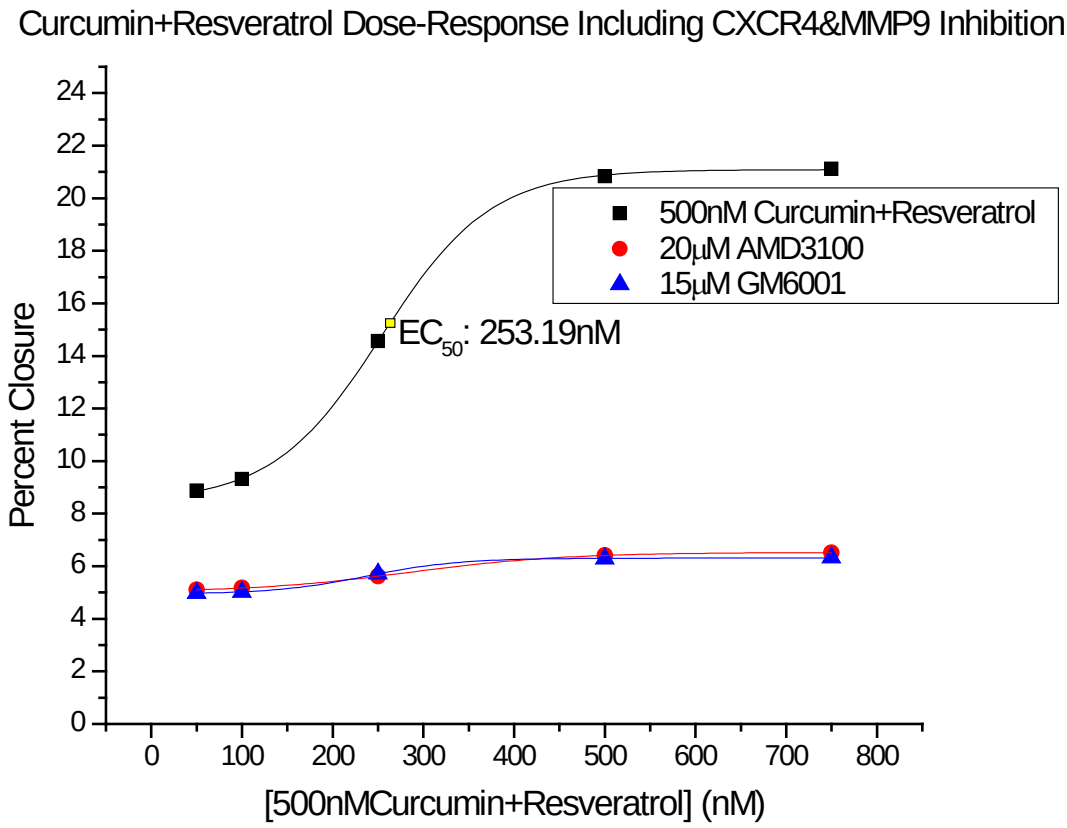

Figure 4 is a line graph representation illustrating migration of CB-MSCs induced by exposure to 500nM curcumin and resveratrol (black sqaures), 500nM curcumin and resveratrol inhibited by CXCR4 inhibitor (AMD3100) (red circles) and 500nM curcumin and resveratrol inhibited by MMP9 inhibitor (GM6001) (blue triangles). Percent closure is plotted as a function of dose and the data was modeled by sigmoidal curve fitting to calculate EC_{50} values. This Figure 4 shows curcumin and resveratrol-induced MSC migration with a calculated EC_{50} of 253.19 nM and maximal migration of the combination of curcumin and resveratrol. The CXCR4 inhibitors showed inhibition of CB-MSC with a closure of 1%. The MMP9 inhibitors also showed inhibition of CB-MSC with a closure of 1%. The results showed a lower EC_{50} than that observed with VPA only, i.e., 32.96 μM suggesting a synergistic effect of CC-Res on CB-MSC migration.

The molecular mechanisms of the effect of lithium and VPA were then investigated on stem cell migration. To understand the effects of nutraceuticals as a replacement to pharmaceuticals, curcumin, quercetin and resveratrol were investigated to compare lithium and VPA results. Since a prior report suggested that VPA up-regulated CXCR4, a critical chemokine receptor involved with cellular mobility, and that lithium up-regulated MMP-9 (Tsai, LK**,** et al., Stroke 42(10): 2932-2939, 2011), the effects of known inhibitors of CXCR4 and MMP-9 on the migration of CB-MSCs were determined and the results are shown in Figure 1, which is a line graph representation illustrating migration of human MSCs exposed to a combination of lithium and VPA with and without inhibition of MMP9 and CXCR4. The data shows the dose-response curve of CB-MSCs treated with Li and VPA alone, treated with Li and VPA and

inhibition of MMP9 by GM6001 (Figure 1) have the same effect with less concentration in the nutraceutical findings (Figure 2 and 3). Percent closure is plotted as a function of dose. The results indicate that the CXCR-4 inhibitor, AMD 3100, blocked the VPA-induced CB-MSC migration, curcumin-induced CB-MSC migration and that GM 6001, a competitive inhibitor of MMP-9, blocked lithium induced CB-MSCs, quercetin induced CB-MSCs, and resveratrol induced CB-MSCs. These results suggest that CXCR4 and MMP-9 are molecular components of the VPA and lithium-induced migration, curcumin and quercetin-induced migration, and curcumin and resveratrol-induced migration of CB-MSCs thus confirming the replacement of these pharmaceuticals with these nutraceuticals.